Hydrogen passivation of poly-Si/SiOx contacts for Si solar cells using Al2O3 studied with deuterium

Hydrogen passivation of poly-Si/SiO_x contacts for Si solar cells using Al_2O_3 studied with deuterium

Manuel Schnabel, Bas W. H. van de Loo, William Nemeth, Bart Macco, Paul Stradins, W. M. M. Kessels, and David L. Young

Citation: Appl. Phys. Lett. **112**, 203901 (2018); doi: 10.1063/1.5031118
View online: https://doi.org/10.1063/1.5031118
View Table of Contents: http://aip.scitation.org/toc/apl/112/20
Published by the American Institute of Physics

Hydrogen passivation of poly-Si/SiO_x contacts for Si solar cells using Al_2O_3 studied with deuterium

Manuel Schnabel,[1] Bas W. H. van de Loo,[2] William Nemeth,[1] Bart Macco,[2] Paul Stradins,[1] W. M. M. Kessels,[2] and David L. Young[1]
[1]*National Renewable Energy Laboratory, Golden, Colorado 80401, USA*
[2]*Department of Applied Physics, Eindhoven University of Technology, 5600 MB Eindhoven, Netherlands*

(Received 28 March 2018; accepted 1 May 2018; published online 14 May 2018)

The interplay between hydrogenation and passivation of poly-Si/SiO_x contacts to *n*-type Si wafers is studied using atomic layer deposited Al_2O_3 and anneals in forming gas and nitrogen. The poly-Si/SiO_x stacks are prepared by thermal oxidation followed by thermal crystallization of a-Si:H films deposited by plasma-enhanced chemical vapor deposition. Implied open-circuit voltages as high as 710 mV are achieved for *p*-type poly-Si/SiO_x contacts to *n*-type Si after hydrogenation. Correlating minority carrier lifetime data and secondary ion mass spectrometry profiles reveals that the main benefit of Al_2O_3 is derived from its role as a hydrogen source for chemically passivating defects at SiO_x; Al_2O_3 layers are found to hydrogenate poly-Si/SiO_x much better than a forming gas anneal. By labelling Al_2O_3 and the subsequent anneal with different hydrogen isotopes, it is found that Al_2O_3 exchanges most of its hydrogen with the ambient upon annealing at 400 °C for 1 h even though there is no significant net change in its total hydrogen content. *Published by AIP Publishing.* https://doi.org/10.1063/1.5031118

The photovoltaic market is currently dominated by crystalline silicon (c-Si) solar cells,[1] with most companies manufacturing diffused homojunction solar cells with ever higher efficiencies. In contrast, the recent burst of c-Si laboratory cell efficiency records above 25.0% has been enabled by a move away from such diffused junctions, over to the so-called passivated or carrier-selective contacts,[2,3] which utilize band offsets and tunneling in addition to doping and band bending to achieve carrier selectivity.[4]

Specifically, doped a-Si:H/intrinsic a-Si:H stacks,[5] and doped poly-Si/SiO_x stacks,[6–9] are commonly employed, with the doped layer used to provide carrier selectivity, while the intrinsic a-Si:H or SiO_x layers provide passivation to the c-Si surface while still allowing for charge transport. The well-passivated surface allows for higher open-circuit voltages than are possible with diffused junctions, and future generations of high-efficiency, large-volume c-Si modules are likely to utilize this technology. A number of groups working on poly-Si/SiO_x contacts apply hydrogenation treatments, such as hydrogen plasma treatments or post-annealed SiN_x:H or Al_2O_3:H coatings, to further improve passivation;[6,9–12] however, it is not entirely clear how this improvement comes about. Al_2O_3:H is a particularly promising hydrogen source as it performed better than a remote hydrogen plasma in our initial trials, is already used in Si PV manufacturing,[13,14] and has other applications in a solar cell, such as enabling local rear contacts. It is therefore of interest to study in detail the passivating mechanism of Al_2O_3:H on poly-Si/SiO_x and the role of hydrogen in the process.

In this letter, we study the interplay between hydrogenation and passivation of *p*-type poly-Si/SiO_x contacts on *n*-type Si wafers, using Al_2O_3:H and anneals in forming gas and nitrogen. Minority carrier lifetime data are compared to secondary ion mass spectrometry (SIMS) profiles of hydrogen, and deuterated alumina (Al_2O_3:D) is used to gain more insight into the hydrogenation chemistry. We achieve implied open-circuit voltages at 1-sun (iV_{oc}) in line with state-of-the-art poly-Si/SiO_x passivated contacts and elucidate the role Al_2O_3 and post-deposition anneals play in achieving excellent passivation.

Symmetric *p*-type poly-Si/SiO_x passivated contact structures were prepared as shown schematically in Fig. 1(a).

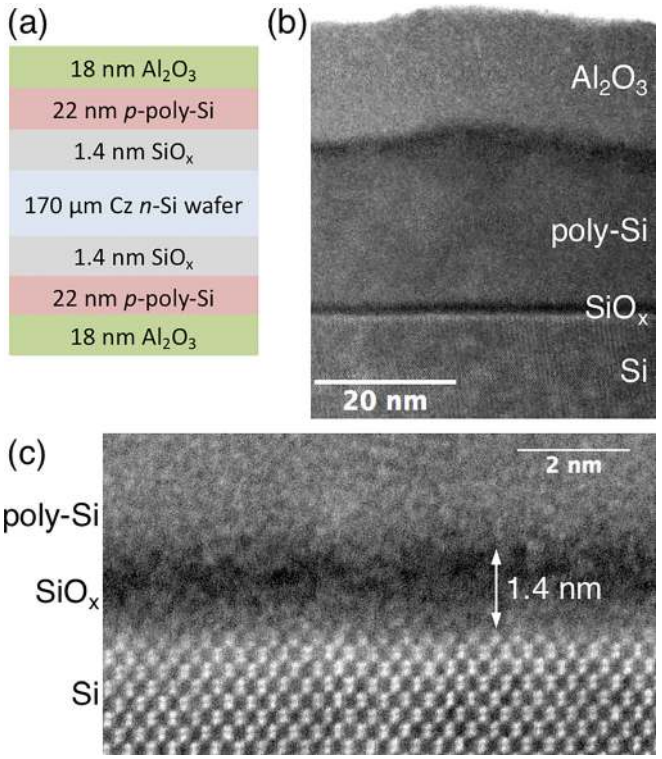

FIG. 1. Schematic (a) and cross-section high-angle annular dark field scanning transmission electron micrographs (HAADF STEM) (b) and (c) of symmetric *p*-type poly-Si/SiO_x samples with Al_2O_3 prepared for this study.

Saw-damage etched 170 μm thick 3 Ω cm *n*-type Czochralski-grown (Cz) (100) Si wafers and single-side polished 400 μm thick 3 Ω cm (100) *n*-Cz-Si wafers were used for lifetime and SIMS measurements, respectively. After RCA cleaning,[15] both types of wafers were oxidized in 6:1 N_2:O_2 at 700 °C for 5 min, resulting in a 1.4 nm thick thermal oxide. Then, ~20 nm boron-doped a-Si:H was deposited on both sides of the wafers by plasma-enhanced chemical vapor deposition and crystallized by annealing in N_2 at 850 °C for 30 min.[9] Due to the consensus in the literature that *p*-type poly-Si/SiO_x contacts tend to be the limiting factor in a solar cell as they exhibit a higher recombination rate than *n*-type poly-Si/SiO_x contacts,[9,11,16,17] we focus on the former.

Some samples were maintained as-crystallized, while others had Al_2O_3:D deposited on both sides by thermal atomic layer deposition (ALD) at 200 °C, using $Al(CD_3)_3$ and D_2O as precursors. SIMS [Fig. 4(a)] showed 10× less hydrogen than deuterium in the bulk of these films but with equal hydrogen and deuterium concentrations at the Al_2O_3:D surface and at the Al_2O_3:D/poly-Si interface. Elastic recoil detection showed a depth-averaged deuterium concentration 2.5× higher than the hydrogen concentration. As-crystallized and Al_2O_3-coated samples were then exposed to 400 °C anneals in nitrogen and/or forming gas (FGA, N_2:10 vol. % H_2) for up to 1 h; some forming gas anneals were performed with deuterated forming gas (99.7% nominal isotopic enrichment). The purpose of using deuterated Al_2O_3 and/or FGA is to separate hydrogen from different sources in SIMS and to take advantage of the much lower SIMS detection limit for deuterium.[18] Minority carrier lifetimes achieved with hydrogen and deuterium treatments were equivalent, and so, hydrogen and deuterium can be considered chemically equivalent within this study.

Photoconductance decay measurements performed with a Sinton WCT-120 lifetime tester were used to measure minority carrier lifetimes and iV_{oc}, which equals the quasi-Fermi level splitting at 1-sun and thus represents an upper limit on solar cell voltage.[19–22] Figure 2(a) shows the results for three representative samples: all curves exhibit the same shape, shifting to higher lifetimes and higher injection levels as passivation improves. Both the saturation current density j_0 and the bulk lifetime τ_b, extracted according to Ref. 23 (see also Ref. 24), improve as iV_{oc} improves, justifying the use of iV_{oc} as the main metric in this letter. Dynamic SIMS was performed using a Cameca IMS 7f instrument with low-energy 1.5 keV O_2^+ primary ions for improved depth resolution, and profiles were quantified with implanted Si standards. This means that absolute hydrogen and deuterium concentrations are only correct within the poly-Si and the c-Si wafer.

Figures 1(b) and 1(c) show high-angle annular dark field scanning transmission electron micrographs (HAADF STEM images) of the layer stack on a polished wafer, acquired with a JEOL ARM200 probe corrected transmission electron microscope, operated at 200 kV. The thermal oxide between the wafer and the poly-Si is indeed 1.4 nm thick and remains almost atomically flat after processing. The poly-Si layer is 22 nm thick on average but exhibits some film thickness inhomogeneity and is conformally coated by Al_2O_3 with a homogeneous thickness of 18 nm. It is therefore likely that the Al_2O_3/poly-Si interface will be sharp in SIMS, whereas the poly-Si/SiO_x interface will be somewhat smeared out.

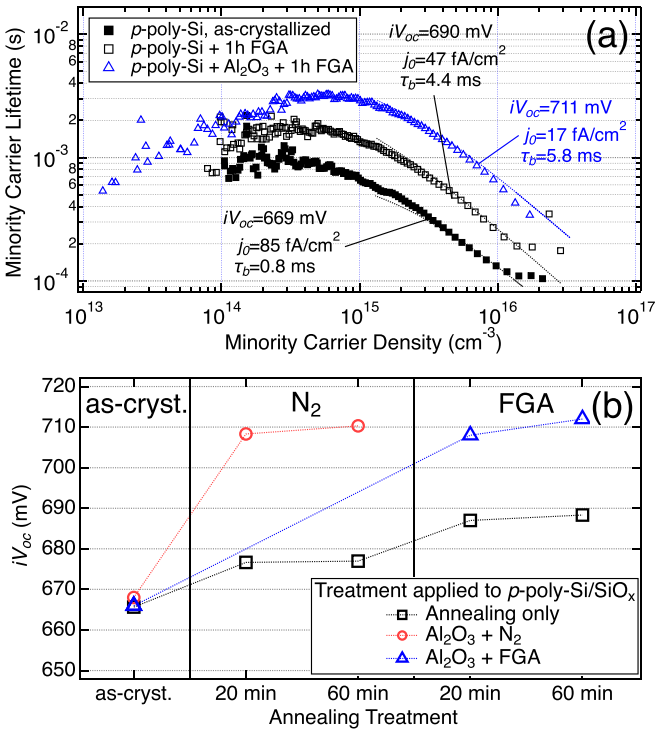

FIG. 2. (a) Representative injection-level dependent lifetime curves along with Kane-Swanson fit lines and iV_{oc}, j_0 (per side), and τ_b values. The labels point to the injection level at 1 sun. (b) Implied open-circuit voltages of symmetric *p*-type poly-Si/SiO_x lifetime samples as a function of annealing treatment (black), Al_2O_3 and N_2 annealing time (red) and Al_2O_3 and FGA annealing time (blue). Lines are guides to the eye, connecting cumulative anneals. Each data point represents the mean of three identically processed samples.

The effects of Al_2O_3 deposition, and N_2 and FGA annealing, on the iV_{oc} of symmetric *p*-type poly-Si/SiO_x samples are shown in Fig. 2(b). Before any treatment, the as-crystallized samples exhibit a mean iV_{oc} of 667 mV. Annealing in N_2 for 20–60 min yields a 10 mV increase, and subsequently annealing in FGA increases iV_{oc} by a further 10–12 mV, suggesting a positive effect of hydrogen on passivation. Depositing Al_2O_3 alone does very little, but deposition of Al_2O_3 and subsequent annealing at 400 °C in N_2 or FGA increases iV_{oc} by 40 mV or more, up to 710 mV. This value compares favorably with champion iV_{oc} values of 691 mV,[17] 696 mV,[10] and 725 mV[25] presented in other recent works on *p*-type poly-Si/SiO_x emitter contacts to *n*-type Si wafers and highlights the efficacy of the annealed Al_2O_3 approach for maximizing the cell voltages that such contacts will allow (also for *n*-type poly-Si/SiO_x[9]).

To determine how hydrogen is involved in these iV_{oc} improvements, SIMS depth profiles were acquired and are shown in Fig. 3. Since hydrogen and deuterium had been found to be chemically equivalent, the sum of H and D concentrations is of interest to understand passivation. In Fig. 3(a), H and D are shown separately because all samples have much more H than D, and so, [H] ≈ [H] + [D], but in Fig. 3(b), [H] + [D] is shown for clarity, with the separation of H and D presented in Fig. 4. The raw oxygen signal is shown as a reference for identifying boundaries between layers.

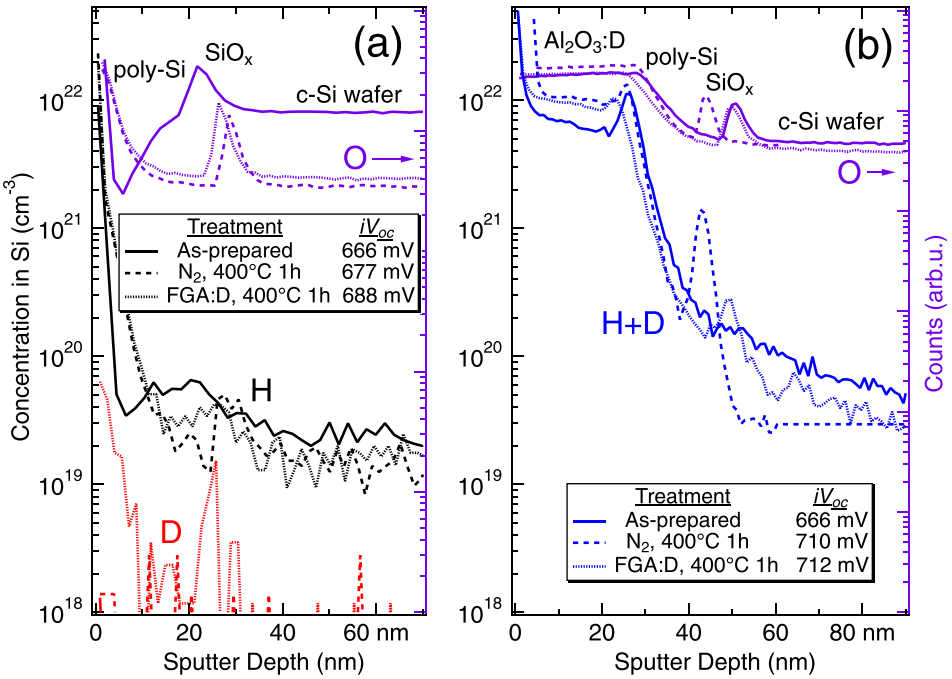

FIG. 3. Hydrogen and deuterium SIMS profiles (left axis) and unquantified oxygen signal (right axis) in *p*-type poly-Si/SiO_x contacts as a function of annealing without (a) and with (b) an Al_2O_3:D layer. For (b), only a summed H + D profile is provided for clarity; isotope effects are shown in Fig. 4. The vertical axes of both panels in this figure are identical.

Figure 3(a) shows that the H profiles of all samples *without* Al_2O_3 exhibit a steep decay in the first 10 nm, which is an artefact attributed to surface adsorbates, as well as a small peak at the position of SiO_x. It is conceivable that SIMS is more sensitive to H in oxides than c-Si, and it is plausible that small amounts of H are present at SiO_x in as-crystallized samples, originating from the a-Si:H precursor deposition. However, these peaks are not particularly pronounced because the SIMS background level for hydrogen is $>10^{19}\,cm^{-3}$ [Fig. 3(a)]. On the other hand, the background level for deuterium is below $10^{18}\,cm^{-3}$. From the deuterium profiles, we see that deuterium is only present at levels exceeding the SIMS background in the sample annealed in deuterated forming gas (FGA:D), revealing an in-diffusion profile at the surface of the poly-Si and a $\sim 10^{19}\,cm^{-3}$ peak at the SiO_x. The use of deuterated forming gas therefore allows us to correlate the 10 mV improvement in iV_{oc} after FGA:D [as compared to N_2 annealing, Fig. 2(b)] with the in-diffusion of hydrogen isotopes from the FGA:D, which was not evident from hydrogen profiles alone. The reason for the 10 mV iV_{oc} improvement upon N_2 annealing is unclear but may be related to in-diffusion of background hydrogen from the ambient.

Turning to the SIMS profiles of samples prepared *with* Al_2O_3 [Fig. 3(b)], it is apparent that deposition of Al_2O_3 at 200 °C alone does not appear to provide any hydrogen or deuterium to SiO_x, whereas a subsequent anneal for 1 h at 400 °C leads to a clear H + D peak. This correlates well with the effect on iV_{oc} and demonstrates that a key way in which Al_2O_3 improves the surface passivation of poly-Si/SiO_x is by acting as a hydrogen source that leads to improved chemical passivation of SiO_x and its interfaces to Si. The peaks also indicate that even though poly-Si itself is also known to contain defects that react with hydrogen,[26,27] enough hydrogen is supplied to overcome the poly-Si and provide some hydrogen to SiO_x. Why the N_2 anneal produces a larger peak than the FGA anneal is not entirely clear, but possible reasons include a thinner poly-Si layer in that sample, allowing more H or D to diffuse through to the SiO_x or a smoother poly-Si in that sample, leading to both H + D and O peaks being higher and narrower.

Effective passivation of bare silicon wafers (without poly-Si) by Al_2O_3 also requires an activating anneal,[28,29] which has been attributed primarily to hydrogen diffusion to the Al_2O_3/c-Si interface, passivating defects; oxygen diffusion to the interface, improving the thin SiO_x interlayer between Al_2O_3 and c-Si; and a negative fixed charge of several $10^{12}\,cm^{-2}$ that yields improved field-effect passivation. Removing Al_2O_3 (with HF) from a *p*-type poly-Si/SiO_x sample annealed in N_2 for 1 h has no effect on iV_{oc}, j_0, and τ_b, indicating that, in contrast to Al_2O_3 passivation of bare Si wafers, field effect passivation from fixed charges in Al_2O_3 was negligible in our samples. This is reasonable as the areal doping concentration of the *p*-type poly-Si is $\sim 10^{14}\,cm^{-2}$, allowing it to screen such a fixed charge in the Al_2O_3 (the Debye length is below 0.5 nm). Diffusion of oxygen to SiO_x, making it more stoichiometric, seems unlikely as any oxygen expelled from Al_2O_3 would probably oxidize the poly-Si instead. We conclude that of the mechanisms proposed to explain activation of Al_2O_3/c-Si passivation, only hydrogen passivation seems to apply to the Al_2O_3/poly-Si/SiO_x/c-Si system.

Comparing hydrogenation from FGA and Al_2O_3 by examining iV_{oc} changes and SIMS profiles [Figs. 2(b) and 3] reveals that the anneals alone had a much smaller effect on passivation and SiO_x hydrogen content than post-annealed Al_2O_3. On the other hand, for post-annealed Al_2O_3, the annealing ambient seems not to be important. To determine how exactly Al_2O_3 interacts with the ambient in which it is annealed, we examine the separate H and D profiles of samples coated with Al_2O_3:D before and after annealing, both in N_2 and in FGA with hydrogen (FGA:H, Fig. 4).

Initially, the as-deposited Al_2O_3:D contains substantially more D than H (except at the surface and interface to the poly-Si, which is tentatively attributed to adsorption before

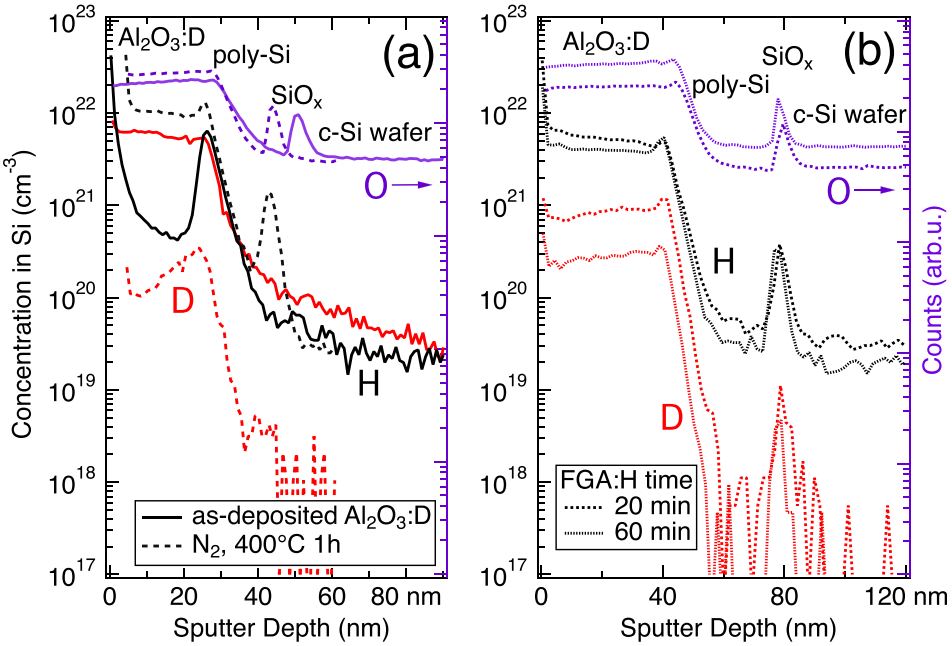

FIG. 4. Hydrogen and deuterium SIMS profiles (left axis) and unquantified oxygen signal (right axis) of *p*-type poly-Si/SiO_x with an Al_2O_3:D layer. (a) Before annealing and after a N_2 anneal at 400 °C for 1 h. (b) After annealing in FGA:H at 400 °C. The vertical axes of both panels in this figure are identical. The elevated D concentration within the wafer for the "as-deposited" dataset in panel (a) is tentatively attributed to knock-on of D from Al_2O_3:D and is not otherwise interpreted.

and after ALD). Once it is annealed, most of the D is lost and replaced with H. In the case of FGA:H annealing, this can be attributed to isotope exchange with H supplied by FGA:H, but in the case of N_2 annealing, the effect is more puzzling and more pronounced. It is tentatively attributed to isotope exchange with species adsorbed on Al_2O_3.

Interestingly, regardless of the origin of the hydrogen that has been exchanged into the Al_2O_3, the isotope ratio at the SiO_x mirrors that within the Al_2O_3, and the total [H] + [D] content changes by less than a factor two upon annealing, indicating that there is little net in-diffusion but rapid isotope exchange at near-constant [H] + [D] [see also Fig. 3(b)]. After annealing, the D profiles in the Al_2O_3 decrease towards the sample surface (sputter depth of 0 nm in Fig. 4), and the H profiles decrease away from it, confirming that isotope exchange occurs at the surface. This isotope labelling experiment reveals that the exchange of hydrogen between the Al_2O_3 and the ambient is rather rapid and that Al_2O_3 excels in delivering both hydrogen it contained, and hydrogen it absorbed, to the underlying layers. The chemistry of hydrogenation from Al_2O_3 upon annealing is thus shown to be more complicated than simple thermally activated diffusion of hydrogen incorporated into Al_2O_3 during growth into the underlying layer.

However, the *net* in-diffusion of hydrogen isotopes from the ambient into Al_2O_3 is small compared to the amount already present in pristine Al_2O_3 [Fig. 3(b)], and, as discussed previously, the net in-diffusion from FGA into poly-Si is small compared to the hydrogen isotopes supplied by Al_2O_3 (Fig. 3). Typical ALD Al_2O_3 contains ~3 at. % hydrogen[29] or $\sim 3 \times 10^{21}\,cm^{-3}$, whereas applying the ideal gas law yields $\sim 1 \times 10^{18}\,cm^{-3}$ H_2 for FGA (at 400 °C). It is therefore entirely possible that Al_2O_3 hydrogenates poly-Si/SiO_x better than FGA simply because it provides a greater volumetric hydrogen concentration. Another factor is that hydrogen in FGA is present as H_2 molecules, whereas hydrogen in Al_2O_3 is present as OH[28] and has been proposed to diffuse through Al_2O_3 as atomic hydrogen.[30] An examination of the literature on MOS devices with poly-Si or Al gates[31] reveals some parallels to our results: poly-Si-gated devices exhibit lower trap densities after annealing in N_2, even more so after FGA, whereas Al-gated devices improve upon annealing irrespective of the ambient. The former is attributed to passivation by H_2 from the ambient or poly-Si grain boundaries, whereas the latter is attributed to a reaction of Al with trace amounts of water at the Al/SiO_2 interface, producing AlO_x and atomic hydrogen that rapidly passivates SiO_2/Si defects (termed "alneal"). Atomic hydrogen also diffuses through poly-Si much more readily than molecular hydrogen,[26] and so, the type of hydrogen present in Al_2O_3 could provide another explanation for its better hydrogenation of SiO_x.

In conclusion, the passivation of *p*-type poly-Si/SiO_x contacts to *n*-type c-Si can be improved by applying an Al_2O_3 layer, followed by post-deposition annealing in N_2 or FGA. This enables iV_{oc} values as high as 710 mV. This improvement remains if the Al_2O_3 is etched off and correlates with hydrogenation of the SiO_x, demonstrating that Al_2O_3 is chiefly a hydrogen source for chemically passivating defects. Al_2O_3 layers hydrogenate poly-Si/SiO_x much better than a forming gas anneal, either because they create a higher volumetric hydrogen concentration at the poly-Si surface or because they supply hydrogen in a form that reaches SiO_x or passivates it more readily. Using isotope labelling, it was shown that Al_2O_3 rapidly exchanges hydrogen with the ambient, even in the absence of a significant net uptake or release of hydrogen. Irrespective of whether its hydrogen originated within it, or diffused into it, Al_2O_3 has been shown to excel at hydrogenating the underlying layers.

We acknowledge the support of Jeff Klein and Vincenzo LaSalvia for sample processing, Matthew Young for SIMS measurements, and John Perkins for elastic recoil detection measurements. Marcel A. Verheijen is acknowledged for performing the TEM studies. Solliance and the Dutch province of Noord-Brabant are acknowledged for funding the TEM facility.

This work was supported by the U.S. Department of Energy under Contract No. DE-AC36-08GO28308 with Alliance for

Sustainable Energy, LLC, the Manager and Operator of the National Renewable Energy Laboratory. Funding was provided by the U.S. Department of Energy Office of Energy Efficiency and Renewable Energy Solar Energy Technologies Office and by TKI Urban Energy from the "Toeslag voor Topconsortia voor Kennis en Innovatie" of the Dutch Ministry of Economic Affairs (AAA Project).

[1]M. A. Green, "Commercial progress and challenges for photovoltaics," Nat. Energy **1**, 15015 (2016).
[2]M. A. Green, Y. Hishikawa, E. D. Dunlop, D. H. Levi, J. Hohl-Ebinger, and A. W. Y. Ho-Baillie, "Solar cell efficiency tables (version 51)," Prog. Photovoltaics **26**, 3–12 (2018).
[3]NREL, *NREL Efficiency Chart* (National Renewable Energy Laboratory, Golden, CO., 2018).
[4]J. Melskens, B. W. H. Van de Loo, B. Macco, L. E. Black, S. Smit, and W. M. M. Kessels, "Passivating contacts for crystalline silicon solar cells: From concepts and materials to prospects," IEEE J. Photovoltaics **8**, 373–388 (2018).
[5]S. De Wolf, A. Descoeudres, Z. C. Holman, and C. Ballif, "High-efficiency silicon heterojunction solar cells: A review," Green **2**, 7 (2012).
[6]F. Feldmann, M. Bivour, C. Reichel, H. Steinkemper, M. Hermle, and S. W. Glunz, "Tunnel oxide passivated contacts as an alternative to partial rear contacts," Sol. Energy Mater. Sol. Cells **131**, 46–50 (2014).
[7]M. Rienäcker, M. Bossmeyer, A. Merkle, U. Römer, F. Haase, J. Krügener, R. Brendel, and R. Peibst, "Junction resistivity of carrier-selective polysilicon on oxide junctions and its impact on solar cell performance," IEEE J. Photovoltaics **7**, 11–18 (2017).
[8]J. Stuckelberger, G. Nogay, P. Wyss, M. Lehmann, C. Allebé, F. Debrot, M. Ledinsky, A. Fejfar, M. Despeisse, F. J. Haug *et al.*, "Passivating contacts for silicon solar cells with 800 °C stability based on tunnel-oxide and highly crystalline thin silicon layer," in *2016 IEEE 43rd Photovoltaic Specialists Conference (PVSC)* (2016), pp. 2518–2521.
[9]B. Nemeth, D. L. Young, M. R. Page, V. LaSalvia, S. Johnston, R. Reedy, and P. Stradins, "Polycrystalline silicon passivated tunneling contacts for high efficiency silicon solar cells," J. Mater. Res. **31**, 671–681 (2016).
[10]F. Feldmann, C. Reichel, R. Müller, and M. Hermle, "The application of poly-Si/SiOx contacts as passivated top/rear contacts in Si solar cells," Sol. Energy Mater. Sol. Cells **159**, 265–271 (2017).
[11]G. Nogay, J. Stuckelberger, P. Wyss, Q. Jeangros, C. Allebé, X. Niquille, F. Debrot, M. Despeisse, F.-J. Haug, P. Löper *et al.*, "Silicon-rich silicon carbide hole-selective rear contacts for crystalline-silicon-based solar cells," ACS Appl. Mater. Interfaces **8**, 35660–35667 (2016).
[12]G. Nogay, J. Stuckelberger, P. Wyss, E. Rucavado, C. Allebé, T. Koida, M. Morales-Masis, M. Despeisse, F.-J. Haug, P. Löper *et al.*, "Interplay of annealing temperature and doping in hole selective rear contacts based on silicon-rich silicon-carbide thin films," Sol. Energy Mater. Sol. Cells **173**, 18–24 (2017).
[13]H. Huang, J. Lv, Y. Bao, R. Xuan, S. Sun, S. Sneck, S. Li, C. Modanese, H. Savin, A. Wang *et al.*, "20.8% industrial PERC solar cell: ALD Al2O3 rear surface passivation, efficiency loss mechanisms analysis and roadmap to 24%," Sol. Energy Mater. Sol. Cells **161**, 14–30 (2017).
[14]D. Pysch, C. Schmitt, B. Latzel, J. Horzel, R. Sastrawan, O. Voigt, B.-U. Sander, S. Patzig-Klein, A. Pediaditakis, S. Queisser *et al.*, "Implementation of an ALD-Al2O3 PERC-technology into a multi- and monocrystalline industrial pilot production," Presented at the 29th European Photovoltaic Solar Energy Conference, Amsterdam, 2014.
[15]W. Kern and D. Puotinen, "Cleaning solutions based on hydrogen peroxide for use in silicon semiconductor technology," RCA Rev. **31**, 187–205 (1970); W. Kern, "The evolution of silicon wafer cleaning technology," J. Electrochem. Soc. **137**, 1887 (1990).
[16]C. Reichel, F. Feldmann, R. Müller, R. C. Reedy, B. G. Lee, D. L. Young, P. Stradins, M. Hermle, and S. W. Glunz, "Tunnel oxide passivated contacts formed by ion implantation for applications in silicon solar cells," J. Appl. Phys. **118**, 205701 (2015).
[17]J. Stuckelberger, G. Nogay, P. Wyss, Q. Jeangros, C. Allebé, F. Debrot, X. Niquille, M. Ledinsky, A. Fejfar, M. Despeisse *et al.*, "Passivating electron contact based on highly crystalline nanostructured silicon oxide layers for silicon solar cells," Sol. Energy Mater. Sol. Cells **158**(Part 1), 2–10 (2016).
[18]F. A. Stevie, C. Zhou, M. Hopstaken, M. Saccomanno, Z. Zhang, and A. Turansky, "SIMS measurement of hydrogen and deuterium detection limits in silicon: Comparison of different SIMS instrumentation," J. Vac. Sci. Technol., B **34**, 03H103 (2016).
[19]F. Feldmann, M. Simon, M. Bivour, C. Reichel, M. Hermle, and S. W. Glunz, "Carrier-selective contacts for Si solar cells," Appl. Phys. Lett. **104**, 181105 (2014).
[20]A. Cuevas and R. A. Sinton, "Prediction of the open-circuit voltage of solar cells from the steady-state photoconductance," Prog. Photovoltaics **5**, 79–90 (1997).
[21]R. A. Sinton, A. Cuevas, and M. Stuckings, "Quasi-steady-state photoconductance, a new method for solar cell material and device characterization," in *Conference Record of the Twenty Fifth IEEE Photovoltaic Specialists Conference—1996* (1996), pp. 457–460.
[22]P. Würfel, *Physics of Solar Cells—From Principles to New Concepts* (Wiley-VCH Verlag GmbH & Co. KGaA, Weinheim, 2005).
[23]D. Kane and R. Swanson, "Measurement of the emitter saturation current by a contactless photoconductivity decay method," in *IEEE Photovoltaic Specialists Conference* (1985), Vol. 18, pp. 578–583.
[24]G. J. M. Janssen, Y. Wu, K. C. J. J. Tool, I. G. Romijn, and A. Fell, "Extraction of recombination properties from lifetime data," Energy Procedia **92**, 88–95 (2016).
[25]U. Römer, R. Peibst, T. Ohrdes, B. Lim, J. Krügener, T. Wietler, and R. Brendel, "Ion implantation for poly-Si passivated back-junction back-contacted solar cells," IEEE J. Photovoltaics **5**, 507–514 (2015).
[26]N. M. Johnson, D. K. Biegelsen, and M. D. Moyer, "Deuterium passivation of grain-boundary dangling bonds in silicon thin films," Appl. Phys. Lett. **40**, 882–884 (1982).
[27]L.-P. Scheller, M. Weizman, P. Simon, M. Fehr, and N. H. Nickel, "Hydrogen passivation of polycrystalline silicon thin films," J. Appl. Phys. **112**, 063711 (2012).
[28]S. Kühnhold, P. Saint-Cast, B. Kafle, M. Hofmann, F. Colonna, and M. Zacharias, "High-temperature degradation in plasma-enhanced chemical vapor deposition Al2O3 surface passivation layers on crystalline silicon," J. Appl. Phys. **116**, 054507 (2014).
[29]G. Dingemans and W. M. M. Kessels, "Status and prospects of Al2O3-based surface passivation schemes for silicon solar cells," J. Vac. Sci. Technol., A **30**, 040802 (2012).
[30]G. Dingemans, F. Einsele, W. Beyer, M. C. M. van de Sanden, and W. M. M. Kessels, "Influence of annealing and Al2O3 properties on the hydrogen-induced passivation of the Si/SiO2 interface," J. Appl. Phys. **111**, 093713 (2012).
[31]M. L. Reed and J. D. Plummer, "Chemistry of Si-SiO2 interface trap annealing," J. Appl. Phys. **63**, 5776–5793 (1988).